JMES The International Journal of
Mechanical Engineering and Sciences
https://iptek.its.ac.id/index.php/jmes
e-ISSN 2580-7471

Studies of the effect of melt spinning on the electrochemical properties of the AB_2 Laves phase alloys

Ika Dewi Wijayanti[1*], Live Mølmen[2], Roman Denys[3], Matylda N. Guzik[4], Stéphane Gorsse[5], Jean-Louis Bobet[5], Volodymyr Yartys[3]

[1]Department of Mechanical Engineering, Institut Teknologi Sepuluh Nopember, Surabaya 60111, Indonesia

[2]Department of Material Science and Engineering, Norwegian University of Science and Technology (NTNU), Trondheim, Norway, 7491

[3]Department of Battery Technology, Institute of Energy Technology (IFE), Kjeller, Norway, 2027

[4]Department of Technology Systems, University of Oslo (UiO), Kjeller, Norway, 2027

[5]Department of Materials Science and Engineering, Univ. Bordeaux, CNRS, Bordeaux INP, ICMCB, UMR 5026, Pessac F, France, 33600

Received: 14 January 2021, Revised: 3 March 2021, Accepted: 9 March 2021

Abstract

A comparative study of the effect of melt spinning on the electrochemical properties of the C14 and C15 AB2 alloys has been performed. The wheel speeds of 630, 2100, and 4100 cm/s were applied during the rapid solidification of both alloys. The structural analysis of the formed phases was performed by X-ray powder diffraction (XRD), while their microstructural morphology was studied by scanning electron microscopy (SEM). In both alloys a tremendous grain refinement due to the melt spinning process was observed: In addition, melt spinning also significantly contributed to the morphological variation of the microstructural changes in C14 alloys which showed changes from the equiaxed grain at lower speed to the small dendrites at higher speed. In contrast to the C14 alloys, the morphological variation was not observed for the C15 alloys. Furthermore, for both C14 and C15 alloys melt-spun at 2100 cm/s the maximum capacities of 435 and 414 mAh/g were achieved, respectively. As both alloys revealed the significant grain refinement due to the melt spinning, an increase in electrochemical capacity was achieved. However, the melt spinning parameters need to be further optimized to improve poor activation behavior of the rapidly solidified alloys.

Keywords: Rapid solidification, melt spinning, Laves phase alloys, electrochemical properties, Ni-MH battery

1. Introduction

Laves phases can adopt hexagonal $MgZn_2$- (C14), hexagonal $MgNi_2$- (C36) and cubic $MgCu_2$- (C15) types of structures [1]. C14 and C15 type intermetallic are often utilized as negative electrodes in Nickel-Metal Hydride (Ni-MH) batteries [2]. While the C14-type alloys usually achieve higher storage capacity and excellent cycle stabilities, the C15 phases reveal the tendency to reach a better high-rate performance and are easier activated [3, 4]. However, an optimization of the performance of both alloys is required to mitigate their shortcomings

Zr-based AB2 type Laves phase alloys have attracted great attention due to their promising application as anode materials in Nickel-Metal Hydride (Ni-MH) batteries [5, 6]. However, a poor activation behavior and insufficient cycle stability of the C14- and C15-type intermetallics, respectively, need to be overcome to allow them reaching an improved performance.

Rapid solidification is one of the techniques used to improve the properties of the alloys by modifying their microstructures, extending solid solubility limits and forming metastable constituent phases, while in turn, enhancing their hydrogen sorption properties [7]. A number of rapid solidification parameters need to be adjusted in order to reach improved performance of the rapidly solidified material. Melt spinning is one of the rapid solidification methods, where a molten metal, pushed from the crucible and ejected through the spinning drum, is rapidly cooled to form a ribbon with a specific atomic structure, which may positively affect the formed material properties [8].

In this study, a comparative overview of the melt spinning effects on C14- and C15-type alloys is presented [9, 10]. The comparison included the analysis of the samples phase compositions, microstructural properties and their electrochemical performances The present study provides a broad overview of the studied melt spun inter-

*Corresponding author. Email: dewi@me.its.ac.id

metallics based on which a general relationship between the applied synthesis technique and the properties of the investigated materials, is established.

2. Experimental method

The prepared Zr-based AB2-type intermetallics got a nominal composition close to $Ti_{0.15}Zr_{0.85}La_{0.03}Ni_{1.2}Mn_{0.7}V_{0.12}Fe_{0.12}$ and crystallised with the C14- and C15-type structures.

Further details concerning the chemical compositions of the studied samples can be found elsewhere [9, 10]. The alloys were prepared by a rapid solidification technique with an Edmund Buehler melt spinner (Institut de Chimie de la Matière Condensée de Bordeaux (ICMCB, France)) with the wheel rotation speeds of 630, 2100, and 4100 cm/s.

The melt-spun samples were manually ground and sieved to the powders with the size of 40 - 60 μm which were used for the electrochemical testing. The sieved powders of smaller than 40 μm were used for the XRD characterization with a D8 Focus Bruker diffractometer (a step size of $0.00157°$ in the range of $10 - 90°$ 2θ). GSAS software was used for the Rietveld refinement analysis [11]. The material microstructure was characterized by a Zeiss Supra-55 VP Field Emission SEM.

The electrochemical characterization was carried out with a three-electrode-based CT 2001 Land Battery Tester,. The test details can be found elsewhere [9–13].

3. Results and Discussion

3.1. Phase sample analysis by PXD

Figure 1. shows the phase compositions of the as-cast and melt-spun samples with the C14- and C15-type alloys as obtained from the Rietveld refinements [9, 10]. For the C14-type alloys, the higher speed of the melt spinner resulted in a larger abundance of the C14 phase which is probably caused by the tendency of the C14 Laves phase to preferably form at higher rotation wheel speeds and higher solidification rates [12]. Such effect is even more pronounces at higher speed of the melt spinner for the C15 phases leading even higher increased abundance.

3.2. SEM characterization

The SEM micrographs of the C14 and C15 alloys can be seen in Figure 2. The results obtained for the as-cast materials confirm formation of two-phase alloys. In the C14-type alloys, the C14 phase becomes the main phase, while C15 phase becomes the main phase in the C15-type alloys. For the initial alloys the grain size in the as-cast alloys was significantly larger for the C14 type intermetallic as compared to the C15 one (15 and 3.5, respectively). This indicates that C14 phase in likely to crystallise at lower temperatures as compared to the C15 one. Further to this, a significant grain refinement was observed for both types of intermetallics in the analysed microstructures of all melt-spun samples. The grain size reduction effect is proportional to the increase of the wheel rotation speed.

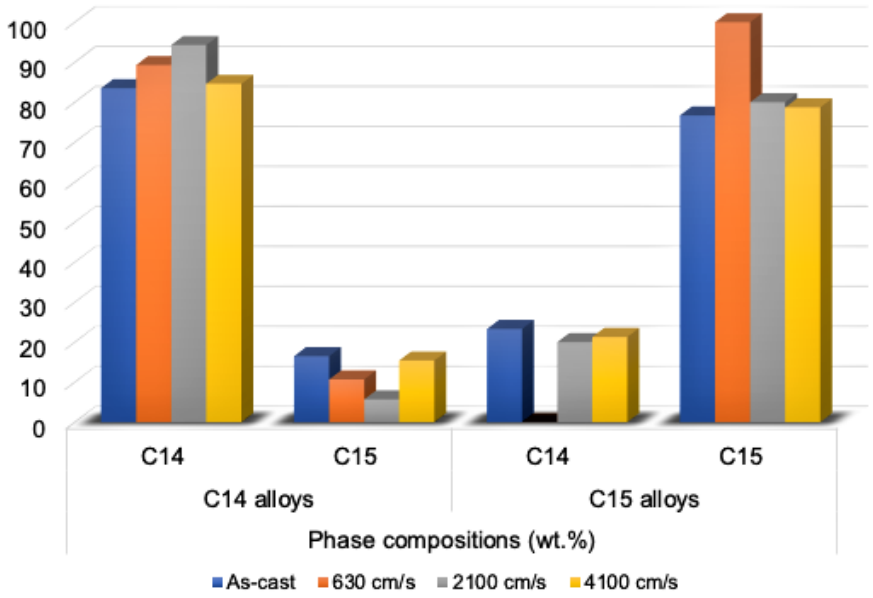

Figure 1. Sample phase compositions based on Rietveld refinement results. The label C14 means that C14 phase as the major phase. Similar, the label C15 means that C15 phase is the major phase.

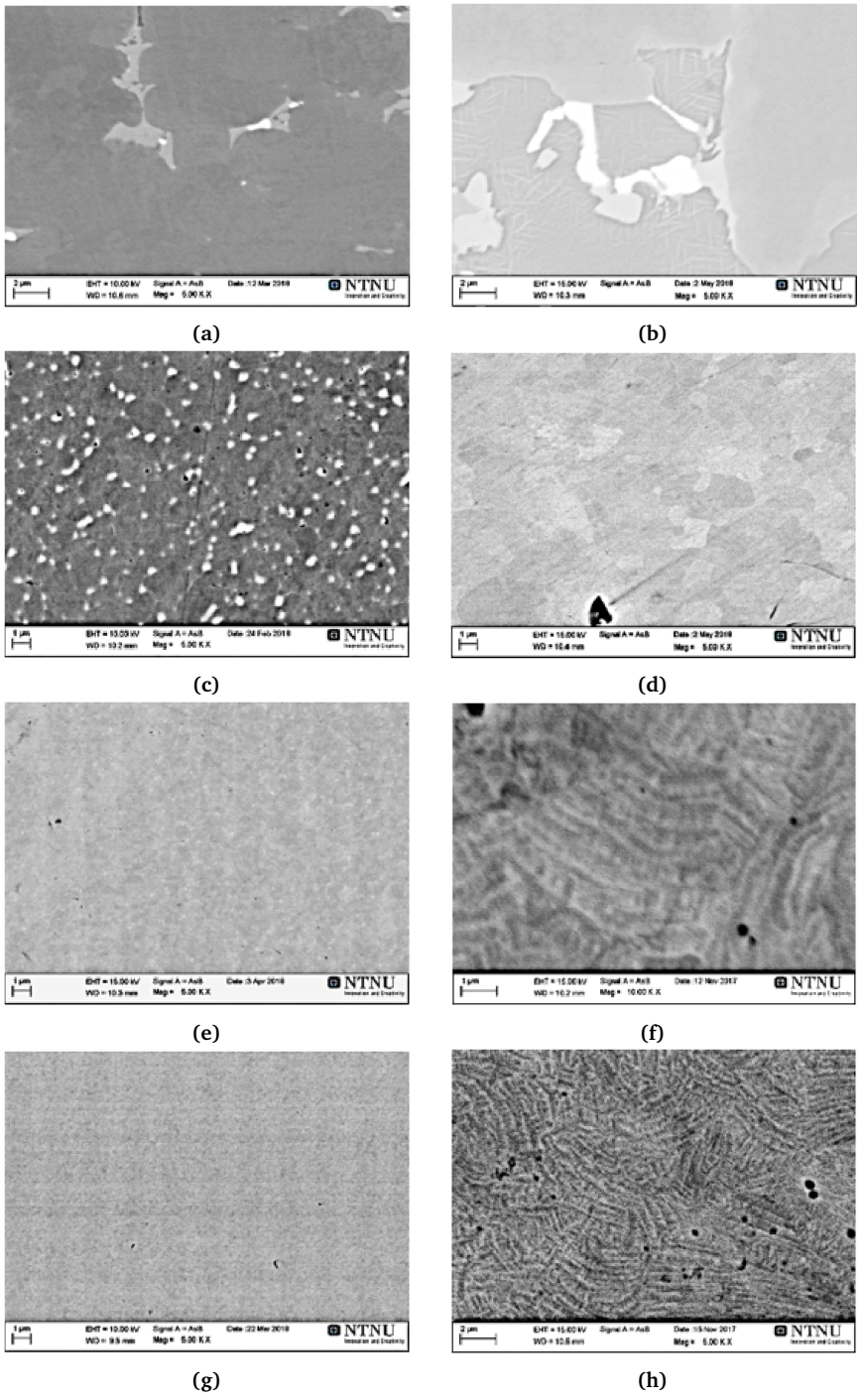

Figure 2. Comparison of microstructural changes in C14 (right: a, b, c, d) and C15 (left: e, f, g, h) alloys prepared as as-cast (a, e), melt-spun alloy at 630 cm/s (b, f), 2100 cm/s (c, g), and 4100 cm/s (d, h).

For C14 melt-spun alloys, when the low speed was applied, the equiaxed grains have been formed. On the other hand, increasing of the speeds, results in forming the dendrites. These dendrites became smaller when the speed increased up to 33 Hz. For C15 melt-spun alloys, there was no change in the microstructural morphology, except of the grain refinement.

Indeed, in the melt-spun C14-type alloys, the grain size refinement resulted in reaching the grain size of 2 mm. This value went down even to the submicron size (0.25 mm) for the C15-type alloys (see Table 1). In addition, melt spinning significantly contributes to the morphological variations among studied samples in C14 alloys, in which the equiaxed grains at lower speed transform to the small dendrite-like regions formed at higher speed. On the contrary, the morphology of the C15 samples remains unchanged for all investigated samples.

Table 1. The relationship between the grain size of the melt-spun alloys and the speed of the spinning wheel [9, 10].

C15-type alloys (μm)				C14-type alloys (μm)			
As-cast	630 cm/s	2100 cm/s	4100 cm/s	As-cast	630 cm/s	2100 cm/s	4100 cm/s
3.5	0.5	0.3	0.25	15	3	2	2

3.3. Electrochemical measurements

The results of electrochemical measurements are listed in Table 2. From the data it is clear that the activation performance of the melt-spun materials appears to be worse than that of the as-cast alloys. Indeed, all samples from the C14 alloys series require more then 10 cycles to get activated, with the material formed at the wheel speed of 4100 cm/s performing the worst. This is in accordance with the previous observations [14], where the increased speed of a melt spinner resulted in a greater abundance of the C14-type, which led to the poorer activation performance of the melt-spun alloys. On the other hand, at the same speed, melt-spun C15 alloys perform better and are able to get activated after 10 cycles. In this case, the reason of the difficult sample activations is likely related to the formation of the thick oxide layer(s) on the alloy surface.

When it comes to the best performance, the maximum energy storage capacity of 435 and 414 mA.h/g for the C14 and C15 alloys, respectively, are reached at the same wheel speed of 2100 cm/s. These values are higher by 8.8 and 31.8% as compared to the numbers obtained for the as-cast C14 and C15 alloy series, respectively.

The A and B melt-spun alloys achieve their best rate performance at the same speed of 2100 cm/s (see Table 2). The smaller decrease in the discharge capacity at the increasing current density is observed for the samples of C15 melt-spun alloy at 2100 cm/s (Figure 3(a)). On the other hand, a significant difference in the discharge capacity of approximately 76% took place for the C14 melt-spun 2100 cm/s alloy (see Figure 3(a)). At the lower current density, the C14 alloys reach higher discharge capacities than the C15 alloys. In contrast to the higher current density, a higher energy storage capacity was obtained by the C14 alloy samples. Indeed, this phenomenon confirms that the C15 alloys achieve a better rate performance compared to the C14 alloys. In addition, the melt spinning process works more effectively in improving the properties of the alloys by achieving the refined phase structures and microstructures in their optimized formation. Therefore, the C15 alloy sample obtained at 2100 cm/s reaches a better rate performance than the corresponding as-cast material, and presents the best rate performance among all investigated alloys (see Figure 3(a)) [9, 10].

When it comes to the comparison of the ate performance of both alloys in terms of potential vs. discharge capacity, the C14 alloys sample processed at a wheel speed of 2100 cm/s shows a dramatic decrease in the discharge capacity, which is pronounced to a much higher extent at the increasing current densities (see Figure 3(c)). As shown in Figure 3(c), longer plateau, wider range, and higher potential vs. discharge capacity values are obtained for the C15 alloy sample melt-spun at 2100 cm/s. At the current density of 300 mA/g the sample energy storage capacity is still at the level of 300 mA.h/g, which indicates that the this material is superior in achieving advanced rate performance.

Table 2. The electrochemical properties of the studied compositions

Electrochemical properties	C14 alloys				C15 alloys			
	As-cast	630 cm/s	2100 cm/s	4100 cm/s	As-cast	630 cm/s	2100 cm/s	4100 cm/s
Activation cycles	14	18	23	26	4	6	11	6
Activation capacity (mAh/g)	267	130	181	208	272	308	306	181
Max. energy storage capacity (mAh/g)	399	420	435	421	314	338	414	195
Increase in energy storage capacity as compared to the as-cast alloys (%)	0	5.3	8.8	5.5	0	7.6	31.8	-37.9

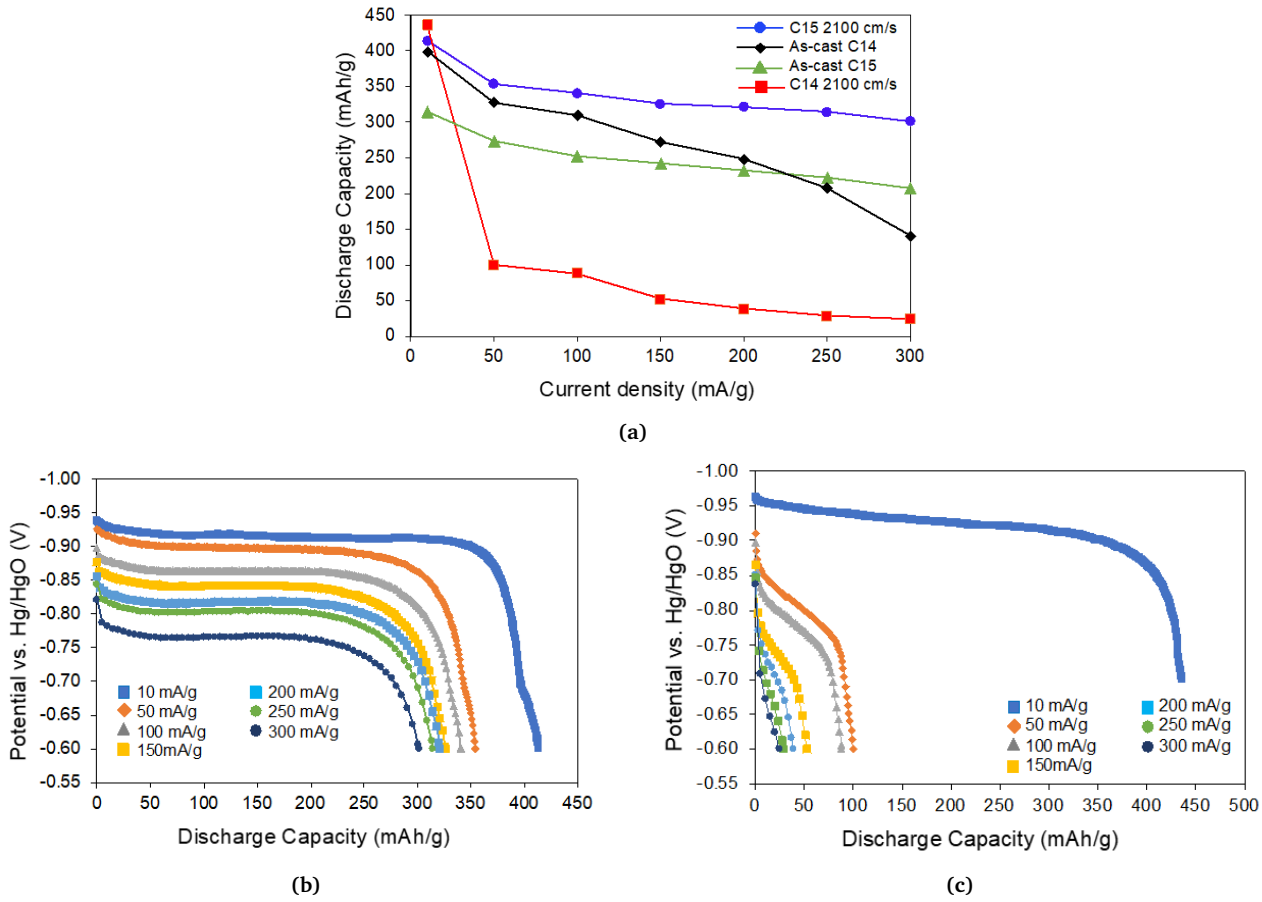

Figure 3. (a) Rate performance of C14 and C15 as-cast alloys and at 2100 cm/s melt-spinner speed, (b) Discharge capacity vs potential plot for C15 melt-spun alloys, (c) Discharge capacity vs potential plot for C14 melt-spun alloys.

4. Conclusions

Melt spinning has been performed on the C14 and C15 alloys with the nominal compositions: $Ti_{0.15}Zr_{0.85}La_{0.03}Ni_{1.2}Mn_{0.7}V_{0.12}Fe_{0.12}$ at a wheel speeds of 630, 2100, 4100 cm/s causing a significant change in the material electrochemical performance as compared to the as-cast samples. Those samples processing resulted in the remarkable grain size refinement optimized phase composition, and modified microstructural state. An excellent value of the maximum discharge capacity above 400 mA.h/g was achieved for each melt-spun alloy series at the same spinning wheel speed of 2100 cm/s. The melt spinning process works effectively in improving the rate performance of the compositions based on the C15-type Laves phases. However, the poor activation performance of the melt-spun alloys requires future optimization of the spinning parameters.

Acknowledgements

Ika Dewi Wijayanti acknowledges with thanks the support from Indonesia Endowment fund for Education (LPDP) during collaboration of a PhD research project between Norwegian University of Science and Technology (NTNU) and Institute for Energy Technology (IFE).

References

[1] K.-H. Young, J. Nei, C. Wan, R. V. Denys, and V. A. Yartys, "Comparison of C14-and C15-predomiated AB2 metal hydride alloys for electrochemical applications," *Batteries*, vol. 3, no. 3, p. 22, 2017.

[2] Y. Liu, H. Pan, M. Gao, and Q. Wang, "Advanced hydrogen storage alloys for Ni/MH rechargeable batteries," *Journal of Materials Chemistry*, vol. 21, no. 13, pp. 4743–4755, 2011.

[3] X. Song, X. Zhang, Y. Lei, Z. Zhang, and Q. Wang, "Effect of microstructure on the properties of Zr-Mn-V-Ni AB, type hydride electrode alloys," *International Journal of Hydrogen Energy*, vol. 24, no. 5, pp. 455–459, 1999.

[4] K. Young, T. Ouchi, B. Huang, B. Chao, M. Fetcenko, L. Bendersky, K. Wang, and C. Chiu, "The correlation of C14/C15 phase abundance and electrochemical properties in the AB2 alloys," *Journal of Alloys and Compounds*, vol. 506, no. 2, pp. 841–848, 2010.

[5] R. Van Essen and K. Buschow, "Composition and hydrogen absorption of C14 type Zr-Mn compounds,"

Materials Research Bulletin, vol. 15, no. 8, pp. 1149–1155, 1980.

[6] J. Bobet and B. Darriet, "Relationship between hydrogen sorption properties and crystallography for TiMn2 based alloys," *International Journal of Hydrogen Energy*, vol. 25, no. 8, pp. 767–772, 2000.

[7] W. . Kurz, B. Giovanola, and R. Trivedi, "Theory of microstructural development during rapid solidification," *Acta Metallurgica*, vol. 34, no. 5, pp. 823–830, 1986.

[8] A. Shirzadi, T. Kozieł, G. Cios, and P. Bała, "Development of Auto Ejection Melt Spinning (AEMS) and its application in fabrication of cobalt-based ribbons," *Journal of Materials Processing Technology*, vol. 264, pp. 377–381, 2019.

[9] I. D. Wijayanti, L. Mølmen, R. V. Denys, J. Nei, S. Gorsse, M. N. Guzik, K. Young, and V. Yartys, "Studies of Zr-based C15 type metal hydride battery anode alloys prepared by rapid solidification," *Journal of Alloys and Compounds*, vol. 804, pp. 527–537, 2019.

[10] I. D. Wijayanti, L. Mølmen, R. V. Denys, J. Nei, S. Gorsse, K. Young, M. N. Guzik, and V. Yartys, "The electrochemical performance of melt-spun C14-Laves type TiZr-based alloy," *International Journal of Hydrogen Energy*, vol. 45, no. 2, pp. 1297–1303, 2020.

[11] A. Larson and R. Von Dreele, *General structure analysis system (GSAS)(Report LAUR 86-748)*. Los Alamos, New Mexico: Los Alamos National Laboratory, 2004.

[12] A. A. Volodin, R. V. Denys, C. Wan, I. D. Wijayanti, B. P. Tarasov, V. E. Antonov, V. A. Yartys, *et al.*, "Study of hydrogen storage and electrochemical properties of AB2-type Ti0. 15Zr0. 85La0. 03Ni1. 2Mn0. 7V0. 12Fe0. 12 alloy," *Journal of Alloys and Compounds*, vol. 793, pp. 564–575, 2019.

[13] I. D. Wijayanti, R. Denys, A. A. Volodin, M. Lototskyy, M. N. Guzik, J. Nei, K. Young, H. J. Roven, V. Yartys, *et al.*, "Hydrides of Laves type Ti–Zr alloys with enhanced h storage capacity as advanced metal hydride battery anodes," *Journal of Alloys and Compounds*, vol. 828, p. 154354, 2020.

[14] K. Shu, Y. Lei, X. Yang, S. Zhang, G. Lü, H. Zhang, and Q. Wang, "Micro-crystalline C14 Laves phase in melt-spun AB2 type Zr-based alloy," *Journal of alloys and compounds*, vol. 311, no. 2, pp. 288–291, 2000.